ELSEVIER

Nuclear Physics B (Proc. Suppl.) 78 (1999) 226–231

NUCLEAR PHYSICS B
PROCEEDINGS
SUPPLEMENTS

www.elsevier.nl/locate/npe

Testbeam results for a shashlik calorimeter with longitudinal segmentation

Presented by F. Terranova.
A.C. Benvenuti[a], I. Britvich[f], T .Camporesi[b], P. Checchia[e], A. Feniouk[f], V. Hedberg[c], V. Lishin[f], M. Margoni[e], M. Mazzucato[e], V. Obraztsov[f], M. Paganoni[d], V. Poliakov[f], F. Simonetto[e], F. Terranova[d], E. Vlassov[f].
[a] Bologna, [b] CERN, [c] Lund, [d] Milano, [e] Padova, [f] Protvino.

A novel technique for longitudinal segmentation of shashlik calorimeters has been tested in the CERN West Area beam facility. A 25 tower e.m. calorimeter has been built with vacuum photodiodes inserted in the first 8 radiation lengths to sample the initial development of the shower. Performance in terms of energy resolution, impact point reconstruction and e/π separation are reported.

1. Introduction

In recent years the "shashlik" technology has been extensively studied to assess its performance at e^+e^-, ep and pp accelerator experiments [1–4]. Shashlik calorimeters are sampling calorimeters in which scintillator light is readout via wavelength shifting (WLS) fibers running perpendicularly to the converter/absorber plates [5,6]. This technique offers the combination of an easy assembly, good hermeticity and fast time response. In many applications it also represents a cheap solution compared to crystals or cryogenic liquid calorimeters.

Shashlik calorimeters are in particular considered to be good candidates for barrel electromagnetic calorimetry at future linear e^+e^- colliders [7]. In this context, the physics requirements impose $\sigma(E)/E \leq 0.1/\sqrt{E(GeV)} + 0.01$, at least three longitudinal samplings, transversal segmentation of the order of $0.9^o \times 0.9^o$ ($\sim 3 \times 3$ cm^2) and the possibility of performing the readout in a 3 T magnetic field. The present shashlik technology can satisfy these requirements, except for the optimization of longitudinal segmentation which still needs development. The solution proposed in this paper consists of vacuum photodiodes inserted between adjacent towers in the front part of the calorimeter. They measure the energy deposited in the initial development of the shower that allows for longitudinal sampling and e/π separation. A prototype has been exposed to a beam with the aim of measuring the sampling capability and of demonstrating that the insertion of diodes neither deteriorates critically the energy response nor produces significant cracks in the tower structure.

2. The prototype detector

The prototype calorimeter that has been tested is made up of 25 Pb/scintillator towers, assembled in a 5×5 matrix. Each tower consists of 140 layers of 1 mm thick lead and 1 mm thick scintillator tiles, resulting in a total depth of $25X_0$. The transversal dimension of each tower is 5×5 cm^2. In the first $8X_0$ the tiles have a smaller transverse dimension to provide room for the housing of the diodes. Plastic scintillator consists of polystyrene doped with 1.5% paraterphenyl and 0.05% POPOP. Optical insulation between the towers is granted by white Tyvek© paper.

The blue light produced in the scintillator is carried to the photodetector at the back of the calorimeter by means of plastic optical fibers doped with green WLS. Two types of fibers have been tested: Bicron BCF20 fibers and Kuraray Y11. In both cases, the emission peak is at about 500 nm. Light collection is increased by aluminizing the fiber end opposite to the photodetector by sputtering. The fibers run through the tiles by means of 1.5 mm holes drilled in lead and scin-

PII S0920-5632(99)00549-6

tillator, uniformly distributed in the tile with a density of 1 fiber/cm^2. All the fibers from the same tower are bundled together at the back and connected to photodetectors.

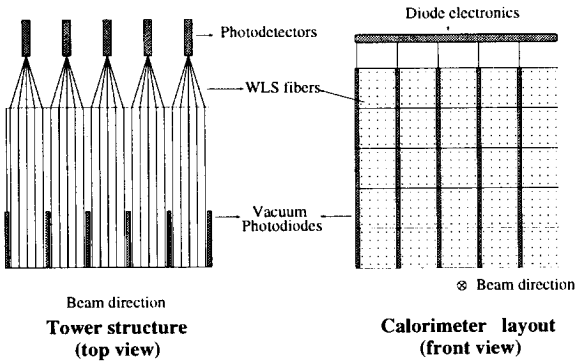

Figure 1. Layout of the calorimeter prototype (not to scale).

The light from the fibers is viewed after a 5 mm air gap by 1" Hamamatsu R2149-03 phototetrodes. Each tetrode is placed inside an aluminium housing, containing a charge sensitive JFET preamplifier and a high voltage divider. In four towers, Hamamatsu Avalanche Photodiodes were installed instead of tetrodes and a plexiglass light guide was used to match the smaller APD sensitive area with the fiber bundle. Preamplifiers and voltage dividers were housed in the same mechanical structure as the tetrodes.

Most of the cells were equipped with EMI vacuum photodiodes [8]. In the present test, 9×5 cm^2 diodes, 5 mm thick, were installed in the first part of the towers in order to sample the energy deposited in the the first 8 X_0, while the readout electronics was positioned above the tower stacks (cfr.fig.1). In addition, a novel diode prototype from Hamamatsu [9], sampling only 4 X_0, was successfully tested in the last part of the data taking period. Technical characteristics of these devices are listed in table 1.

Table 1
Technical characteristics of vacuum photodiodes.

	EMI	Hamamatsu
Sensitive area	28.9 cm^2	10.9 cm^2
Capacitance	250 pF	17 pF
Working bias	-10 V	-20 V
Diode thickness	5.0 mm	5.1 mm

3. Testbeam setup

The prototype was tested in June and September of 1998 at the X5 beam in the CERN West Area. Electrons ranging from 5 to 75 GeV and pions at 10, 20, 30 and 50 GeV were used. The prototype (CALO in fig.2) was installed on a moving platform whose position was controlled at the level of $\simeq 220$ μm. In order to avoid particles from channeling through fibers or diodes, the calorimeter was tilted by 3 degrees in the horizontal plane. The absolute impact position of the incoming particle was measured by means of two Delay Wire Chambers (DWC1 and DWC2) with a 2 mm wire pitch and a spatial resolution of 200 μm, positioned at 0.5 and 1 m from the calorimeter front-face. An external trigger was provided by a layer of scintillators (S) installed near DWC2 while two threshold Cherenkov counters (C1 and C2) were used to determine particle contamination in e and π beams.

A calibration of each tower was carried out exposing the calorimeter to a 50 GeV electron beam at the beginning of each of the two data taking periods. Pedestal runs were taken periodically to test the noise of the electronic amplification chain.

4. Energy resolution

The calibration coefficients were extracted by minimizing the following quantity

$$\sum_{i=1}^{N_{events}} \left(\sum_{j=1}^{N_{towers}} c_j S_{ij} - E_{beam} \right)^2 \qquad (1)$$

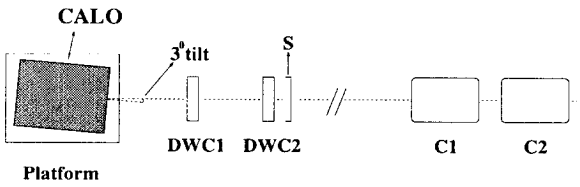

Figure 2. Top view of the testbeam setup (not to scale).

where c_j is the calibration coefficient for tower j and S_{ij} the pedestal subtracted signal in tower j for the event i. The energy response is expected to depend on the impact point since the light collection efficiency is higher close to the fiber. A high fiber density was used in order to reduce the non uniformity in light response to a level of a few percent. This was, however, not achieved with BCF20 fibers, due to a small scintillating component in the fibers which deteriorated the energy resolution. KY11 fibers, on the other hand, allow reduction of non uniformity down to $\pm 1.5\%$. The drop in energy response at the border between the towers was around 4%. The energy resolution achieved with KY11 fibers and tetrode readout is shown in fig.3 and can be parameterized as follows

$$\frac{\sigma(E)}{E} = \left(\frac{9.6\%}{\sqrt{E}} + 0.8\%\right) \oplus \frac{0.127}{E} \qquad (2)$$

where E is expressed in GeV. The last term corresponds to the electronic noise contribution and has been measured from pedestal runs.

The use of phototetrodes as readout media is not ideal for barrel calorimetry at e^+e^- colliders. Tetrodes have a rather long longitudinal dimension and must be kept at a small angle with respect to the magnetic field in order to operate adequately. The installation of Avalanche Photodiodes as an alternative solution has been proposed by the CMS collaboration [10]. Four APD's were installed in the prototype, as described in section 2, and have shown an energy resolution compa-

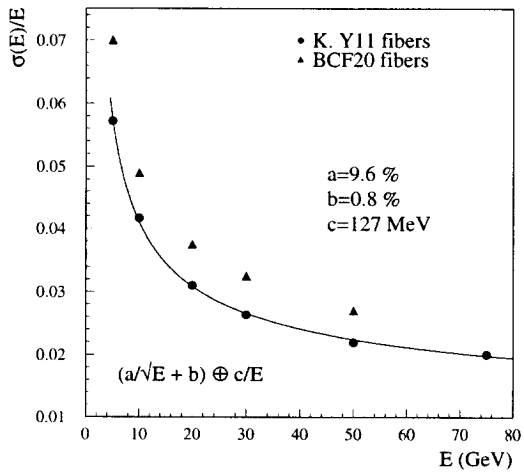

Figure 3. Energy resolution.

rable to that of tetrodes. In fig.4 the energy response for 50 GeV electrons is shown. The small high energy tail comes from events reconstructed near the BCF20 fibers. The tail disappears for towers with KY11 optical fibers. Fig.5 shows the energy response for 50 GeV electrons in towers equipped with Kuraray fibers and tetrode redout.

5. Spatial resolution

A position scan along the towers was done using 50 GeV electrons to establish the precision in the impact point reconstruction. The position reconstruction algorithm is based on the sharing of the deposited energy between nearby calorimeter towers.

As a starting point, the shower center of gravity can be used to estimate the impact position:

$$X_b = 2\Delta \sum_i iE_i / \sum_i E_i \qquad (3)$$

where Δ is the half-width of the tower and E_i the energy deposited in tower i. Non linearities due to the exponential shower profile can bias X_b and,

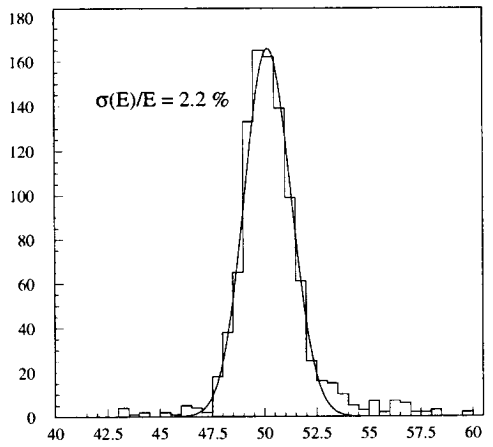

Figure 4. Energy resolution for 50 GeV electrons using an APD as photodetector.

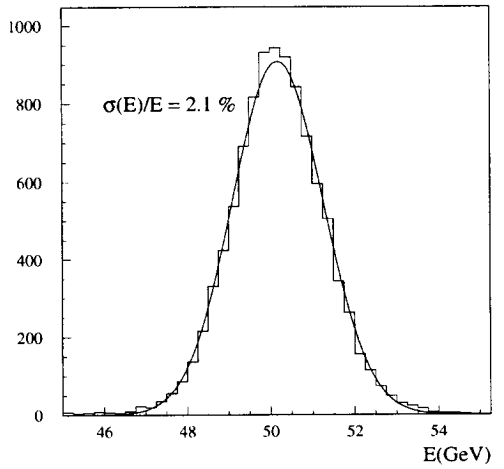

Figure 5. Energy resolution for 50 GeV electrons using tetrode readout and KY11 optical fibers.

following [11], this estimator has been modified according to

$$X_c = b \operatorname{arcsinh}\left(\frac{X_b}{\Delta}\sinh\delta\right) \tag{4}$$

where b is a parameter describing the transversal shower profile ($b = 0.7$ cm) and $\delta \equiv \Delta/b$. X_c is well behaved in most of the impact point range, showing non-linearities only near the diode housing as depicted in fig.6. The non linear behaviour around the diode can be restored using the diode signal itself. In particular, in the range of X_c close to the distortion region, a diode-based estimator can be introduced so that

$$X' = X_c + X_d \tag{5}$$

where

$$X_d = -b' \log\frac{1}{2}\left(1 + \frac{E^{diode}_{max}}{E_{max+1}}\right) + c' \ ; \tag{6}$$

here E^{diode}_{max} is the diode energy in the tower with maximum signal, E_{max+1} represents the energy (seen by tetrodes/APDs) in the tower closest to the maximum and parameters b' and c' depend on geometry and the shower development and are obtained from the testbeam data. Figure 6 shows the effect of the diode correction on the distribution of the reconstructed versus true impact position. The true impact point was measured by DWC1 and DWC2.

The position resolution of the prototype at the center of a cell was 1.6 mm with 50 GeV electrons.

6. e/π separation

Separation of electrons from pions was performed using discriminating variables based either on purely calorimetric data (CALO standalone) or involving also external information like the beam energy or, in a real experimental environment, the momentum estimated from tracking. In the latter case, the fraction

$$\chi_T = \frac{E_{cal}}{E_{beam}} \tag{7}$$

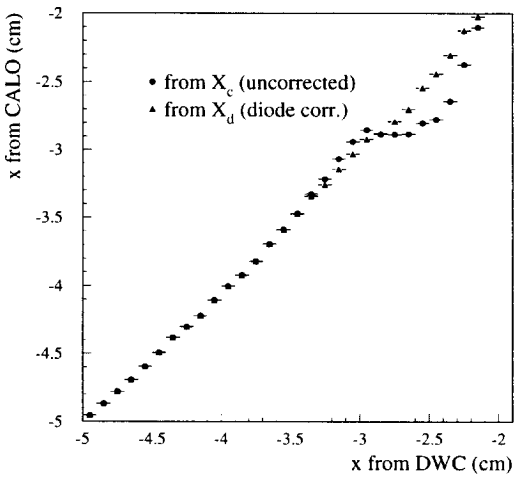

Figure 6. Reconstructed horizontal impact position versus the true one (from DWC). X_c is estimated with eq.(4) and X_d with eq.(5).

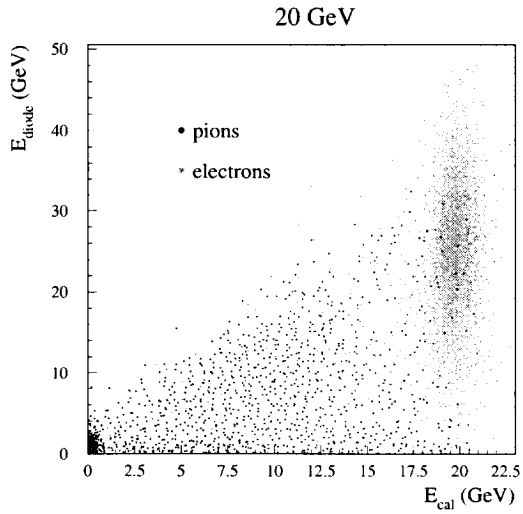

Figure 7. Diode energy versus total tetrode energy for e and π at 20 GeV.

can be combined with standalone variables like the fraction of energy seen by the diodes

$$\chi_D = \frac{E_{diode}}{E_{cal}} \tag{8}$$

and the lateral development of the shower

$$\chi_S = \frac{\sum_{i=1}^{N} E_{cal}^i r_i^2}{\sum_{i=1}^{N} E_{cal}^i} \tag{9}$$

where N is the number of towers with signal, r_i the distance of the tower from the reconstructed impact position and E_{cal}^i the energy deposited in tower i.

Fig.7 shows E_{diode} versus E_{cal} for pions and electrons at 20 GeV. The discriminating power of the different variables in terms of pion contamination for 90% electron efficiency, at energies ranging from 10 to 50 GeV is shown in fig.8. In most of the cases, CALO standalone variables improve the overall separation capability with a factor ~ 2 compared with χ_E by itself.

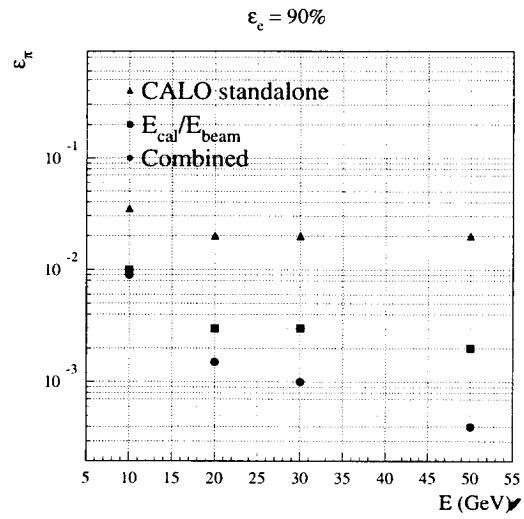

Figure 8. Pion contamination versus energy for 90% electron efficiency.

7. Conclusions

The present test has demonstrated the technical feasibility of longitudinally segmented shashlik calorimeters in which lateral sampling is performed by vacuum photodiodes. Due to the small dimension of the diodes and to the tilt of fibers and diodes with respect to the incoming particles, no significant cracks or dead zones are introduced. Performance in terms of energy resolution, impact point reconstruction and e/π separation seem to be adequate for applications at future e^+e^- collider experiments.

8. Aknowledgements

We wish to thank all the staff and technical support of the SL-EA group for the smooth operation of the accelerator during the testbeam. In particular, we thank L. Gatignon and J. Spanggaard of the SL division for their help in the preparation of the testbeam setup. We would like to thank the technical staff of our home institutes for their excellent work. In particular, we gratefully aknowledge the help we received from V. Giordano and G. Rampazzo.

The contribution of all the IHEP workshop staff has been essential for the construction of the prototype: we are greatly indebted with A. Kleschov, P. Korobchuk and A. Tukhtarov.

REFERENCES

1. J. Badier et al., Nucl. Instr. and Meth. **A348** (1994) 74
2. HERA-B Design report, DESY/PRC 95-01.
3. LHCb Technical proposal, CERN/LHCC 98-4.
4. S.J. Alsvaag et al., CERN/EP 98-132.
5. H. Fessler et al., Nucl. Instr. and Meth. **A240** (1985) 284.
6. G.S. Atoyan et al., Nucl. Instr. and Meth. **A320** (1992) 144.
7. R. Brinkmann, G. Materlik, J. Rossbach, A. Wagner (eds.), DESY 1997-048.
8. EMI vacuum photodiode prototype D437.
9. Hamamatsu vacuum photodiode prototype SPTXC0046.
10. CMS Technical Proposal, CERN/LHCC 94-38
11. G.A. Akopdjanov et al., Nucl. Instr. and Meth. **140** (1977) 441.